ISSN 8756-6990, Optoelectronics, Instrumentation and Data Processing, 2018, Vol. 54, No. 2, pp. 187–202. © Allerton Press, Inc., 2018.
Original Russian Text © N.A. Pakhanov, V.M. Andreev, M.Z. Shvarts, O.P. Pchelyakov, 2018, published in Avtometriya, 2018, Vol. 54, No. 2, pp. 93–112.

PHYSICAL AND ENGINEERING FUNDAMENTALS OF MICROELECTRONICS AND OPTOELECTRONICS

State-of-the-art Architectures and Technologies of High-Efficiency Solar Cells Based on III–V Heterostructures for Space and Terrestrial Applications

N. A. Pakhanov[a,*], V. M. Andreev[b], M. Z. Shvarts[b,], and O. P. Pchelyakov[a]**

[a] *Rzhanov Semiconductor Physics Institute, Siberian Branch, Russian Academy of Sciences, prosp. Akademika Lavrent'eva 13, Novosibirsk, 630090 Rissia*
[b] *Ioffe Physical-Technical Institute, Russian Academy of Sciences, ul. Politekhnicheskaya 26, St. Petersburg, 194021 Russia*
[*] *E-mail: pakhanov@isp.nsc.ru*
[**] *E-mail: shvarts@scell.ioffe.ru*

Received October 23, 2017

Abstract—Multi-junction solar cells based on III–V compounds are the most efficient converters of solar energy to electricity and are widely used in space solar arrays and terrestrial photovoltaic modules with sunlight concentrators. All modern high-efficiency III–V solar cells are based on the long-developed triple-junction III–V GaInP/GaInAs/Ge heterostructure and have an almost limiting efficiency for a given architecture — 30 and 41.6% for space and terrestrial concentrated radiations, respectively. Currently, an increase in efficiency is achieved by converting from the 3-junction to the more efficient 4-, 5-, and even 6-junction III–V architectures: growth technologies and methods of post-growth treatment of structures have been developed, new materials with optimal bandgaps have been designed, and crystallographic parameters have been improved. In this review, we consider recent achievements and prospects for the main directions of research and improvement of architectures, technologies, and materials used in laboratories to develop solar cells with the best conversion efficiency: 35.8% for space, 38.8% for terrestrial, and 46.1% for concentrated sunlight. It is supposed that by 2020, the efficiency will approach 40% for direct space radiation and 50% for concentrated terrestrial solar radiation. This review considers the architecture and technologies of solar cells with record-breaking efficiency for terrestrial and space applications. It should be noted that in terrestrial power plants, the use of III–V SCs is economically advantageous in systems with sunlight concentrators.

Keywords: architectures and technologies of III–V solar cells, III–V/Si solar cells, III–V/Si-Ge-Sn solar cells, multi-junction solar cells, subcells, metamorphic layers.

DOI: 10.3103/S8756699018020115

INTRODUCTION

A simple solar cell (SC) (Fig. 1) includes one p–n junction which separates photogenerated minority charge carriers (electrons and holes) and produces a potential difference (photo-electromotive force). Figure 1a schematically shows the mechanisms of charge carrier losses that affect the efficiency of sunlight conversion by SCs, the main of which is the thermalization of charge carriers (mechanism *2*). Currently, single-junction GaAs SCs have an efficiency of 28.8 % (AM1.5G) [1]. For comparison, the most common Si based SCs show an efficiency close to the theoretical limit of 26.7 % (AM1.5G). The atmosphere mass (AM) is the path length of light through the atmosphere (when the Sun is in zenith, AM = 1).

A significant increase in the SC efficiency was achieved with the advent of multi-junction (MJ) (cascade) architectures formed from several p–n junctions connected in series by tunnel diodes. The main reason for

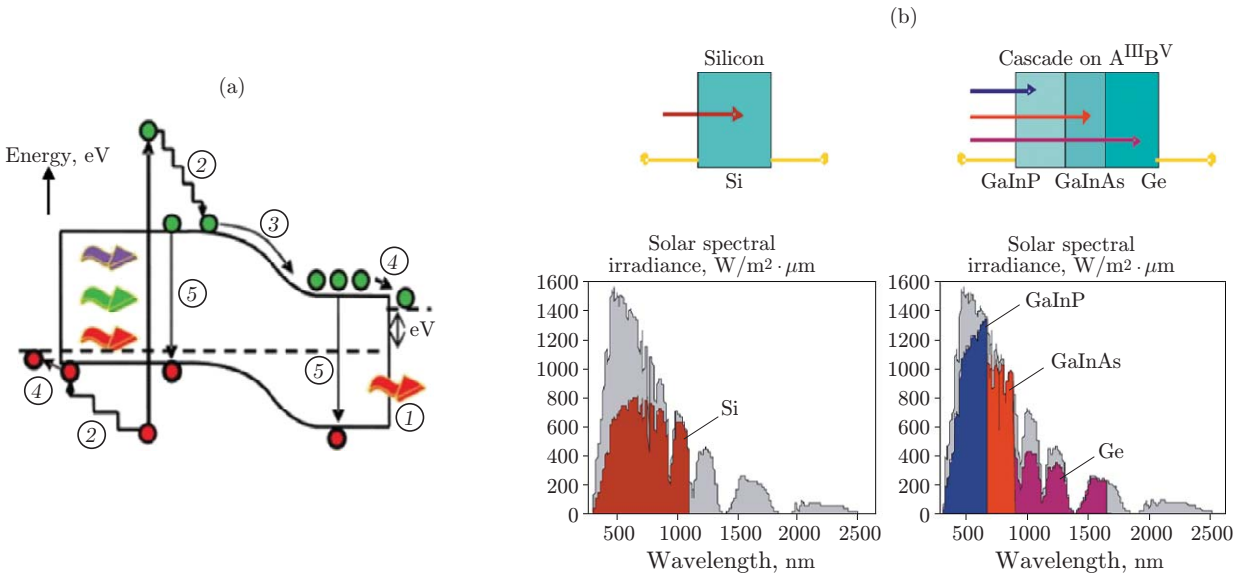

Fig. 1. (a) energy scheme of a standard p–n junction (*1*) is the subzonal passage, (*2*) thermalization, (*3*) loss in the p–n junction, (*4*) loss at contacts, (*5*) recombination); (b) increase in the fraction of the solar spectrum radiation converted by SCs in conversion from the single-junction (Si) to the triple-junction (GaInP/GaInAs/Ge) architecture.

the higher efficiency for multi-junction SCs compared to single-junction ones is a significant decrease in the thermalization energy losses due to a reduction in the difference between the energy of the absorbed photons and the bandgap (BG) width (E_g) of the cascade (Fig. 1b). Therefore, the efficiency of a MJ SC depends primarily on the selection of the optimal combination of the BGs of semiconductor materials and the number of p–n junctions contained in the SC. The concept of multi-junction SCs is most successfully implemented on the basis of the compounds of the III-rd and V-th groups of the Mendeleev Periodic Table (Ga-In-P, Ga-As, and Ga-In-As).

In MJ SCs, the resulting short-circuit photocurrent (I_{sc}) is determined by the lowest photocurrents generated by subcells (p–n junctions). Therefore, in designing the architecture of high-efficiency MJ SCs, they should be matched, i.e., equalized at the highest possible level for the selected structure. The open-circuit voltage (V_{OC}) of a MJ SC is equal to the sum of the voltages of its p–n junctions. Furthermore, the photocurrent depends linearly on the irradiance (at concentrated sunlight conversion, on the concentration ratio (C), and the voltage depends on it logarithmically. The SC efficiency is given by the formula $\mathrm{Eff} = I_{sc}V_{OC}FF/E_CS$, where FF is the fill factor of the current-voltage (I-V) characteristic, E_C is the solar irradiance, and S is the SC area.

Depending on SC applications, the efficiency is determined for the following standard conditions [2]: 1) simulation of the AM0 space spectrum with an irradiance of 1367 W/m^2 [3]; 2) simulation of the total (direct and diffuse) AM1.5G terrestrial solar flux with an irradiance of 1000 W/m^2; 3) simulation of the AM1.5D direct terrestrial solar spectrum with an irradiance of 1000 W/m^2 [4, 5].

TECHNOLOGIES USED IN THE DESIGN OF HIGH-EFFICIENCY SCs BASED ON III–V COMPOUNDS

Let us consider the main technologies for III–V SCs which have been actively developed by the research community. Most efforts have been directed toward increasing the CS efficiency; however, innovative approaches have also been proposed to reduce their specific weight and cost. An example is the replacement of expensive Ge or GaAs substrates by much cheaper, stronger, and lightweight Si substrates.

The overwhelming majority of structures for up-to-date high-efficiency MJ SCs are produced by metal-organic vapor-phase epitaxy (MOVPE) on high-performance commercial reactors. p type germanium is used as an active substrate on which a triple-junction (3J) lattice-matched ((LM) $Ga_{0.50}In_{0.50}P/Ga_{0.99}In_{0.01}As/Ge$ (hereinafter, GaInP/GaInAs/Ge) heterostructure of high crystalline quality is formed. n-type emitters in Ge are obtained by diffusion. Series connection of junctions is provided by low-resistance and optically transparent tunnel diodes.

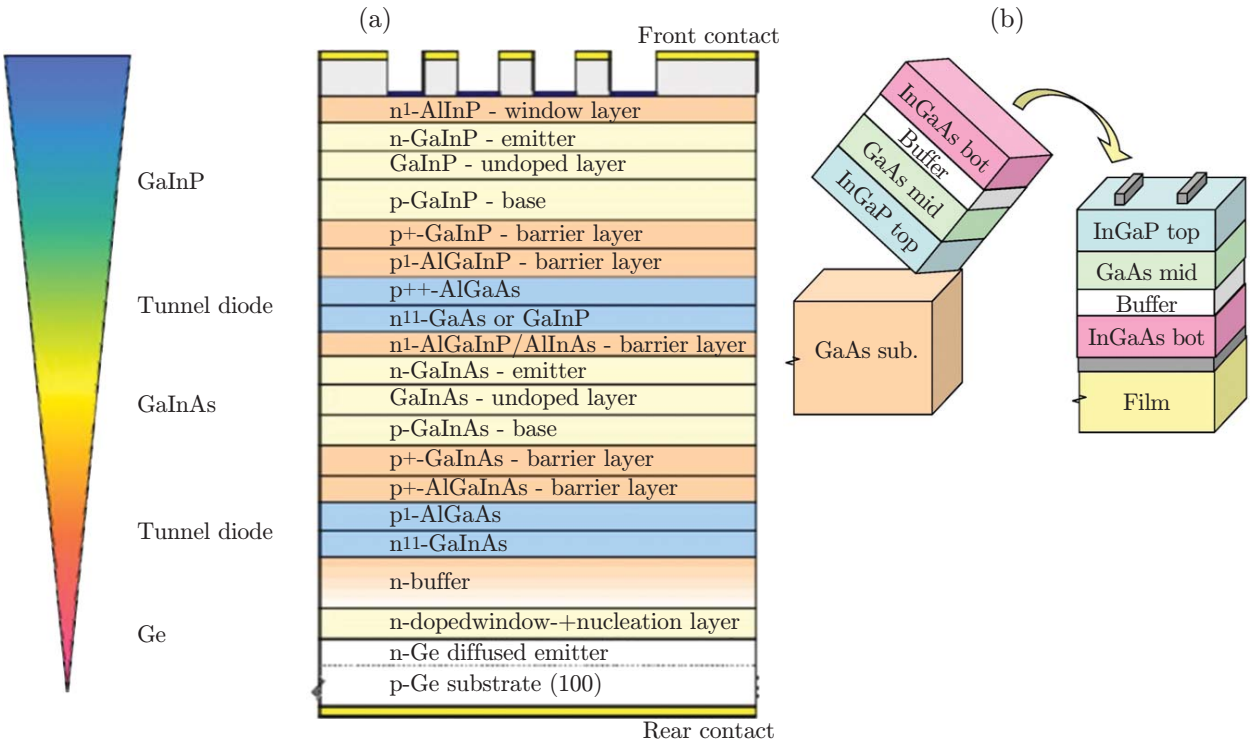

Fig. 2. (a) 3J LM GaInP/GaInAs/Ge SC architecture [6], (b) principle of SC fabrication by IMM growth [7].

In the high-performance LM triple-junction GaInP/GaInAs/Ge heterostructure (Fig. 2a), each layer is optimized for composition, doping level, and thickness [6]. However, the combination of BGs for subcells is not optimal: the bottom Ge narrow-bandgap p–n junction of generates much higher current than each of the GaInP and GaAs subcells. The part of the sunlight energy corresponding to the excess photons absorbed in Ge is uselessly lost, limiting the efficiency of the MJ SC. It is for this reason that a significant increase in the efficiency for a 3J SC with a germanium substrate should not be expected. Current research aimed at improving the efficiency of MJ SCs focus on increasing the number of p–n junctions based on materials with optimal combinations of the E_g values.

Estimates show that the efficiency of 3J SCs can be substantially increased by replacing the narrow-bandgap Ge subcell by a wider-bandgap subcell based on a GaInAsN solid solution lattice-matched to GaAs with E_g in the range 0.7–0.75 eV with the prospect of approaching $E_g \sim 1$ eV [8]. Further increase in the SC efficiency is achieved by including additional narrow-bandgap cascades with E_g in the range 0.7–0.5 eV in the structure. However, the production of such materials has become possible only recently.

CURRENT DIRECTIONS OF RESEARCH

New architectures, design, growth, and post-growth approaches have been developed to increase the efficiency of sunlight conversion. They can include the choice of substrate, the type of epitaxial technology, the concept of growth sequence and post-growth treatment (bringing the structure to a ready device). Combinations of these options give a wide range of opportunities for the implementation of various designs and solutions.

Since the wide-bandgap GaInP/GaInAs tandem (1.86 eV/1.41 eV) technology is well established, it is commonly used as the basis for designing 3- and 4-junction SCs. Efforts are mainly focused on developing narrow-bandgap subcells, i.e., on searching for materials with a BG width smaller than that of GaAs (E_g = 1.41 eV).

Therefore, efforts have been made to replace active Ge (with p–n junction) by more effective, stronger, and lighter element, e.g., a silicon substrate [9–11]. However, because of the large difference in lattice constants and thermal expansion coefficients, it has so far not been possible to obtain GaAs/Si layers of the required quality by direct epitaxial growth [11]. Promising results have been demonstrated within the direct bonding technology of III–V heterostructures with Si wafers [10–13]. Impressive success has been achieved in the

inverted growth of a monolithic 4J-architecture with two metamorphic GaInAs layers with E_g equal to 1 and 0.7 eV [14]. Breakthrough results in bringing the new class of GaInAsNSb solid solutions to instrument quality have been obtained by molecular beam epitaxy (MBE) [8, 15]. Depending on the nitrogen content, the BG width in these compounds can be varied from 1.3 to 0.7 eV with full matching to the GaAs or Ge lattice, which opens up the possibility of fabricating 4-, 5- and even 6-junction SCs with record-breaking efficiency. In addition, ternary group IV Si-Ge-Sn solid solutions for narrow-bandgap subcells are currently developed. The combination of these three elements will make out possible to obtain GaAs and Ge lattice-matched compounds with a BG width of 0.5 to 1.2 eV [16].

In the development of advanced high-efficiency MJ SCs, the following basic techniques and technologies are used.

Upright Metamorphic Growth (UMM)

This is the monolithic growth of several crystals with different crystal lattices, as a rule, in the direction from narrow-bandgap to wide-bandgap subcells. To provide acceptable crystallographic quality of photoactive layers, it is common to use intermediate compensating (buffer) layers with a smoothly changing lattice constant [17, 18].

Inverted Metamorphic Material Growth (IMM)

In this growth, a MJ SC structure is formed starting from a wide-bandgap subcell lattice-matched to the substrate with a transition to narrow-bandgap metamorphic material layers (Fig. 2b) [19–23]. An advantage of this approach over the upright metamorphic structure is that the growth of metamorphic (lattice-mismatched) layers is implemented at later stages of the epitaxial process, which allows fabricating perfect wide-bandgap subcells. It is possible to select an optimal BG width for narrow-bandgap subcells as they are not related to the growth substrate. Then the structure is detached from the substrate (epitaxial lift-off (ELO) technology) and transferred to a new carrier (see Fig. 2b).

Thin layers of MJ SCs are separated from a massive lattice-matched substrate by selective etching in hydrofluoric acid along the sacrificial layer (usually an AlGaAs layer) specially formed during the structure growth. The selectivity of etching along the sacrificial layer relative to the neighboring GaAs layers reaches 10^6. After separation, the epitaxial film is transferred onto a new supporting substrate that can be thin, flexible, ultra-lightweight and with better thermal conductivity than the growth substrate [24]. The original substrates can be used several times, which significantly reduces the cost of produced wafers. Because of the extremely small thickness of the structures, the power/mass ratio of the standard and flexible SCs is greatly improved.

Wafer Bonding Technology

The wafer bonding technology for MJ SCs consists in combining wafers grown separately on different substrates. This provides a wide choice of growth substrates and eliminates the need to use buffer layers compensating the change in the lattice constant along the growth direction of the metamorphic structure. Usually, one of the wafers is formed by IMM growth. The wafers are then bonded together, followed by the removal of one of the substrate using ELO technology. This process of fabricating MJ SCs is complex and requires high technological culture [12, 13, 25–28]. The highest efficiency of MJ SCs was achieved using combined "IMM + bonding" technology and are 46.1 % for 4J GaInP/GaAs//GaInAsP/GaInAs (C = 312, AM1.5D) SCs [29]; 30.2% for 3J GaInP/AlGaAs//Si (C = 1, AM1.5G) SCs [30]; 35.8% (C = 1, AM0) and 38.8% (C = 1, AM1.5D) for 5J SCs [31].

ULTRA-LIGHTWEIGHT RADIATION-HARD $Ga_{0.50}In_{0.50}P/Ga_{0.99}In_{0.01}As$/Ge 3J-UMM SCs

Among the leaders of the space market are the GaInP/GaInAs/Ge 3G30C-Advanced SCs developed by the AZUR Space Solar Power GmbH [32] to ensure maximum radiation resistance. They have a beginning-of-life (BOL) efficiency of 29.5% which reduces to 28.1% (AM0, 1367 W/m^2) at the end of life (EOL), i.e., under irradiation by 1 MeV electrons with a $5 \cdot 10^{14}$ e/cm^2 fluence. The 3G30-Advanced SCs are available in 4×8 cm, 8×8 cm and 6×12 cm configurations with a thickness of 145 μm, have welded contact tapes, a double-layer antireflection coating, and protective glass 50 to 150 μm thick. Since one of the most important parameters of space SCs is weight (the contribution of the Ge substrate is up to 95% of the SC weight), to remove the main part of the Ge substrate, the AZUR Space has developed its own combined chemical-mechanical thinning process, whose details are not published and disclosed [32]. An independent technology

(a)

Cell thickness [μm]	Cell mass [μm]	Cover thickness [μm]	SCA mass [mg/cm^2]
145	84	100	114
145	84	80	108
80	49	100	79
80	49	80	74
50	33	100	63
50	33	50	50
20	17	150	60
20	17	100	47
20	17	50	34

(b)

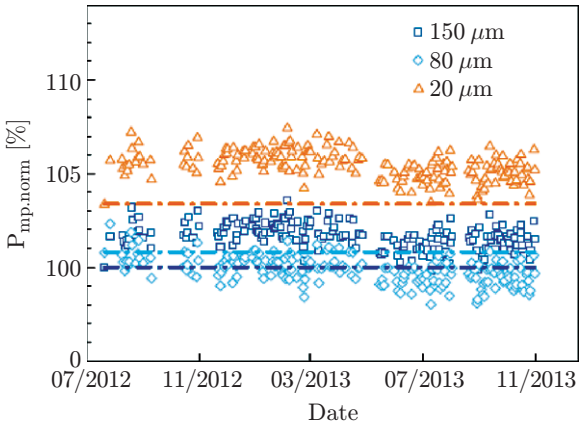

Fig. 3. (a) weight parameters of SCs using different glass sheets (SCA); (b) orbital monitoring data for $P_{\text{mp. norm}}$ values for 3G30-Advanced SCc of various thicknesses [32].

for fabricating ultrathin SCs based on $A^{III}B^{V}$/Ge heterostructures was proposed in [33]. Figure 3a shows the weight parameters of SCs, including those with protective glass, depending on the residual thickness of the SC [8]. Decreasing the SC thickness to 50–20 μm leads to a weight saving of about 45–60 %. Thinned 3G30 SCs passed successful tests on the TET-1 technological satellite (Germany) in the period from 22.07.2012 to 31.10.2013. The data of a 15-month monitoring of the maximum power $P_{\text{mp. norm}}$ for SCs of three types are shown in Fig. 3b. It should be noted that the thinnest (20 μm) SCs have the greatest resistance. Thus, the power output and operational advantages of thin and lightweight GaInP/GaInAs/Ge SCs have been demonstrated.

To further increase the efficiency, the AZUR Space company has developed upright metamorphic growth for 4J-UMM SCs with an a BOL efficiency of 33%. For this, an additional metamorphic buffer layer with a lattice mismatch of no more than 1.5% of Ge is included in the structure, and the BG width for top junctions is increased by adding Al. The top subcells with AlGaInP/AlGaInAs (1.9-eV)/(1.4 eV) architecture and the bottom subcells with GaInAs/Ge (1.1 eV)/(0.7 eV) architecture were obtained by the UMM approach. In the next generation of 4J-UMM SCs from AZUR Space, an EOL efficiency of 30% is expected.

METAMORPHIC 4J SCs FOR SPACE APPLICATIONS

Today, one of the most advanced technologies for designing space SCs with an efficiency above 30 % is inverted metamorphic growth. The leaders in the development of this direction is the Sharp Corporation (Japan) and the Emcore company (since 2014 the SolAero Technologies Corp., U.S.) [14]. To achieve high efficiency, developers use architectures with metamorphic buffer layers and the optimal combination of bandgaps. The architecture of the fourth-generation 4J-IM SC produced by Emcore is shown in Fig. 4a [34]. The main layers and the change in the lattice constant along the growth direction are shown schematically. The diagram relating the lattice parameters and the E_g values for optoelectronic III–V materials shows the transitions from structures lattice-matched to GaAs (GaInP and GaAs) to metamorphic (GaInAs based) structures in the IMM growth of 4J wafers (Fig. 4b).

Significant efforts have been made to optimize the gradient metamorphic buffer layers between GaAs, GaInAs (1 eV), and GaInAs subcells (0.7 eV). These layers are a source of threading dislocations (TDs). Optimization of metamorphic buffers between GaAs (5.65 Å) and 1 eV GaInAs (5.77 Å) has made it possible to reduce the TD density below $5.0 \cdot 10^6$ cm^{-2}, which was a decisive factor for increasing the efficiency. Another resource that has been successfully used to improve the efficiency of 4J-IMM SCs has been the optimization of the substrate removal technology across the separation (sacrificial) layers with subsequent etching treatment. The obtained device demonstrates outstanding photovoltaic parameters for the AM0 irradiation conditions (Fig. 5a). The high quality of the layers of the structure is confirmed by the external quantum efficiency (EQE) of the photoresponse for subcells: the photogenerated carrier collection efficiency in them approaches 100 % (Fig. 5b). Isotype structures with one active p–n junction and inactive adjacent cells with the same general architecture have been grown to analyze and optimize the performance of in-

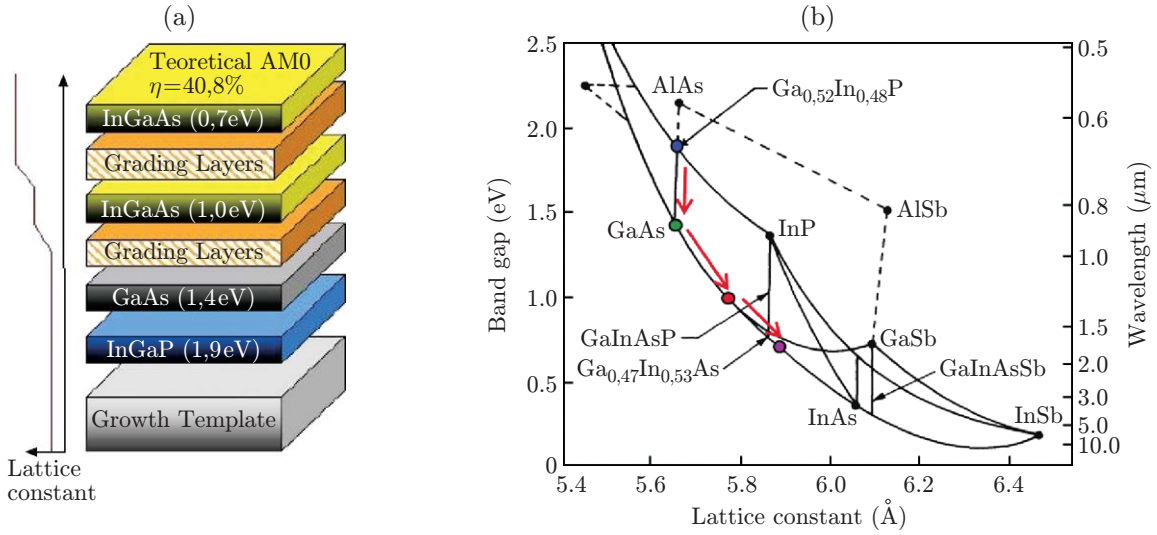

Fig. 4. (a) 4J IMM architecture with an indicator of the change in the lattice constant along the growth direction [14]; (b) diagram of the change in E_g in passing from GaInP and GaAs to metamorphic GaInAs based subcells [34] (large points show the main materials used in 4J IMM, arrows show the direction of growth from the GaInP structure to the GaAs structure and then to two subcells based on InGaAs metamorphic materials).

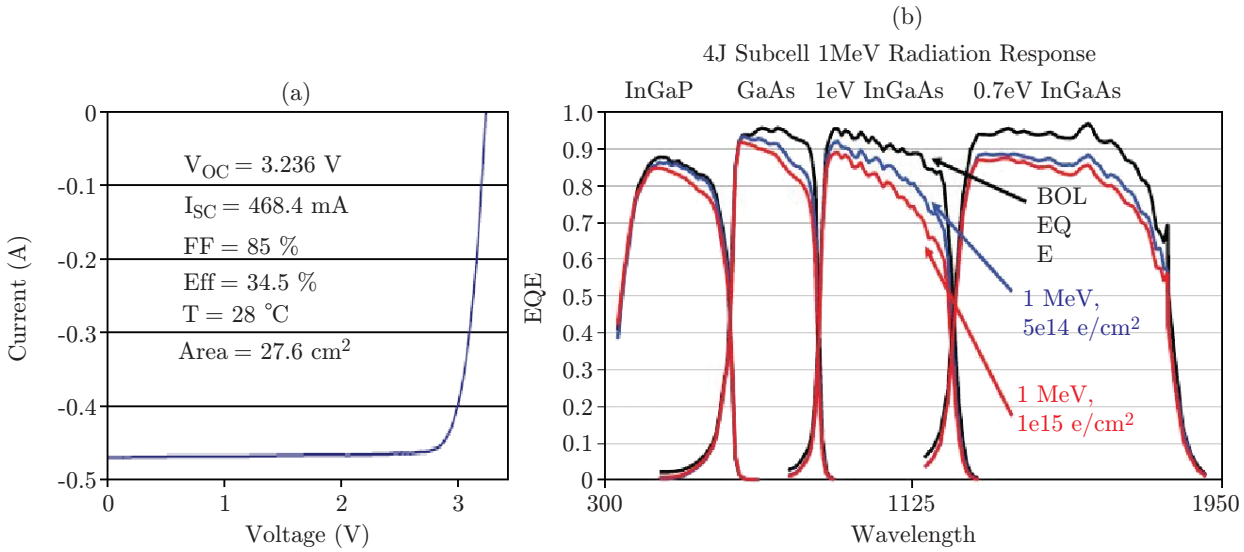

Fig. 5. (a) load I-V curve for 4J-IMM SC; (b) photosensitivity degradation under 1 MeV electron irradiation [14].

dividual subcells.Measurements on active layers have shown that V_{OC} agree with the best literature data. Given the high V_{OC} values, the obtained efficiency of SCs is close to the maximum for this architecture.

Another key parameter of space SCs is the radiation resistance to fluxes of high-energy particles (protons and electrons). The change in EQE upon irradiation with 1 MeV electrons as a function of fluence is shown in Fig. 5b. The first two subcells in the 4J-IMM SCs consist of lattice-matched GaInP and GaAs. The effect of electron and proton irradiation on these materials has been widely studied using commercial GaInP/GaAs/Ge SCs [35]. The estimates of their potential lifetime obtained by the Emcore company can be considered the standard (reference) one for modern space cells. The second two subcells of 4J-IMM SCs are based on GaInAs. Studies have shown that GaInAs subcells are less resistant to damaging particles than GaInP and GaAs samples [36]. The EOL/BOL degradation coefficients obtained for narrow-bandgap GaInAs subcells were used for general optimization of the radiation resistance of the 4J-IMM structure. The optimization was carried out by the end-of-life (EOL) current matching criterion. To obtain the desired

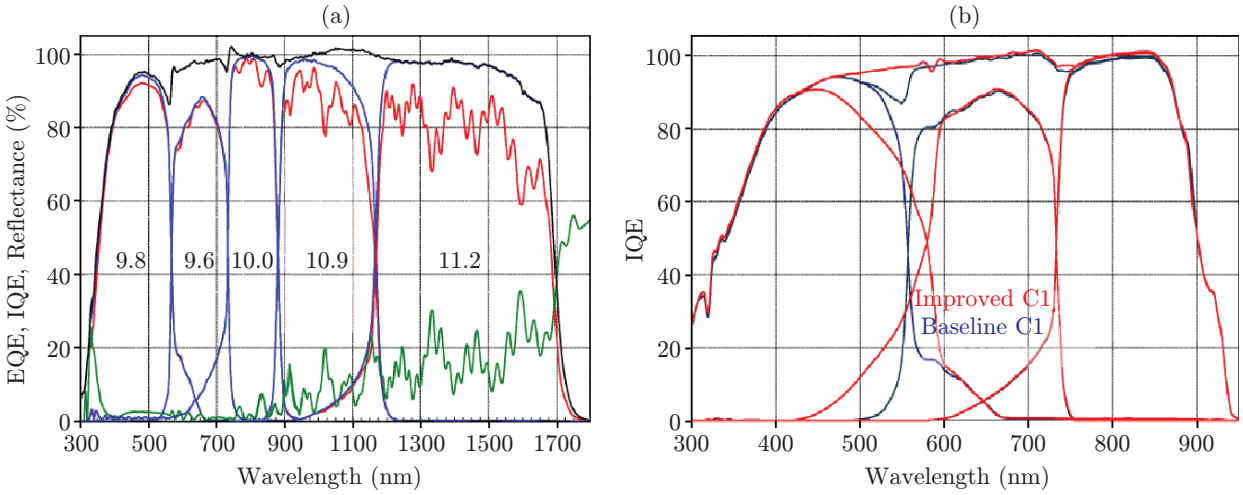

Fig. 6. (a) spectral dependences of EQE, IQE, and the reflection coefficient for a terrestrial 5J SC; (b) improvement in the photosensitivity in the zone of overlapping of the IQE dependences for the first and second subcells [31].

current mismatch at the beginning of life (BOL), the GaInP layer was thinned, E_g in both GaInAs subcells was slightly decreased (see Fig. 4a), and the antireflection coating was tuned for the irradiated structure. As a result, a BOL efficiency of 34% (AM0) and a degradation ratio of EOL/BOL = 0.82 were obtained.

In April 2016, 4J-IMM SCs with a record-breaking efficiency of 32% for commercial SCs and EOL/BOL = 0.85 were released on the space market by the SolAero Technologies Corp. Currently, 4J-IMM SCs have been going through AIAA-S111-2014 qualification tests [37]. In [34], it is reported on the achievement of an efficiency of 46.7% for C = 250 (AM1.5D) in InGaP/GaAs/InGaAs/InGaAs (1 eV)/(0.7 eV) 4J SCs; however this value has not been confirmed independently [1].

FIVE-JUNCTION SCs WITH AN EFFICIENCY OF 35.8% (AM0) AND 38.8% (AM1.5G)

The Spectrolab Inc. (U.S.) demonstrated a 2.2/1.7/1.4/1.05/0.73 eV 5J SC in which the top three subcells (see Fig. 4a) were obtained by the IMM process on a GaAs substrate with the subsequent direct bonding with two cascades with E_g = 1.05 and 0.73 eV formed on an InP substrate [31]. After bonding, the GaAs growth substrate was removed and the 5J-structures were subjected to post-growth processing. An advantage of this approach is that all the subcells making up the monolithic 5J SC are grown lattice-matched to the substrate, providing excellent epitaxial quality of photoactive layers. In particular, each of the narrow-bandgap subcells grown on InP has higher V_{OC} values than on samples based on metamorphic structures or nitride solid solutions [38]. Optimization was carried out for the parameter $W_{oe} = E_g/q - V_{OC}$, which characterizes the shift of the voltage V_{OC} with respect to the BG width of the subcell material. The obtained low W_{oe} values for narrow-bandgap subcells have made it possible to raise the efficiency of 5J SCs to record values of 35.8 % (AM0) and 38.8 % (AM1.5G) for samples with an area of 4 and 1 cm^2 respectively [31]. The V_{OC} values are almost identical for both types of 5J SCs (about 4.76 V) since the differences in thickness and E_g between their constituent subcells are insignificant. Measured photocurrents of 12.12 mA/cm^2 (AM0) and 9.56 mA/cm^2 (AM1.5G) are agree within 1% with the values estimated from measured spectral photosensitivity (Fig. 6a).

Analysis shows the possibility of further increasing the efficiency for space and terrestrial 5J SCs. In particular, there are pronounced valleys in the spectral dependence of the internal quantum efficiency (IQE) in the zone between the first AlGaInP and the second AlGaInAs subcells (see Fig. 6a). Improvement in the quality of wide-bandgap materials allows a marked increase in IQE (Fig. 6b) and hence a rise in the current and voltage of the 5J SC with an expected efficiency increase of 1 abs.%.

Simultaneously with improving the epitaxy in the 2.2/1.7/1.4 eV 3J SC configuration, Spectrolab Inc.has continued to improve the bonding process. For GaAs and InP structures on 4-inch substrates, high bonding quality (nearly void-free) was obtained, and the wafer bonding strength was improved by a factor of 7. It is expected that these improvements will significantly increase the reproducibility of the bonding process, reliability, and efficiency of SCs.

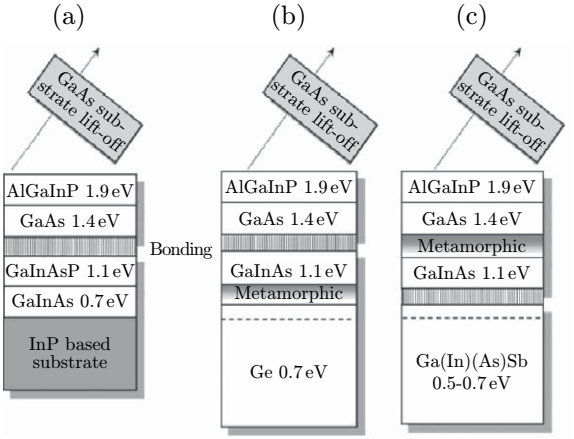

Device concept	η [%]	V_{oc} [V]	J_{sc}/C [mA/cm^2]	FF [%]
InP-based cell (a)	53.8	4.376	14.2	86.7
Ge-based cell (b)	49.5	4.170	13.8	86.2
GaSb-based cell (c)	51.5	4.412	13.4	86.9

Fig. 7. 4J SC architectures formed on InP (a), Ge (b), and GaSb (c) substrates and a table of their calculated photovoltaic parameters at C = 500 [29].

FOUR-JUNCTION SCs WITH NARROW-BANDGAP SUBCELLS ON InP, Ge AND GaSb SUBSTRATES

Currently, the Fraunhofer Institute for Solar Energy Systems (FhG-ISE) is developing the next generation of 4J SCs for the purpose of achieving an efficiency of 40% for direct space and 50 % for concentrated sunlight [29]. Figure 7 shows the architectures of three 4J SCs with a standard top AlGaInP/GaAs cascade and different narrow-bandgap subcells, including those formed on InP, Ge, and GaSb substrates for subsequent bonding. The predicted efficiencies taking into account the practical power losses at C = 500 for all three SCs are in the range of 49–54% (see the table in Fig. 7).

All the conceptual solutions for 4J SCs presented in Fig. 7 have been implemented experimentally. At the FhG-ISE, III–V structures were grown by IMM on InP, GaAs, and Ge substrates and InP structures were grown on a GaAs substrate 100 mm in diameter and a GaSb substrate 50 mm in diameter. InP-GaAs wafers were manufactured by SOITEC and obtained by transferring a thin InP layer (<1 μm) detached from a bulk crystal onto a GaAs wafer using the patented process from the CEA-LETI company [39]. All other SCs were joined via the bonding process in an Ayumi SAB-100 vacuum chamber, in which surface oxides are removed by a beam of fast argon atoms. This technology provides strong surface bonding (10 kN) and an interface resistance of 1–5 $\Omega \cdot \text{cm}^2$. After bonding, the GaAs substrate was removed by chemical etching from the top cascade, and front contacts and an antireflection coating were applied. The SC area was 5.3 mm^2. The photovoltaic parameters of SCs were measured by the FhG-ISE laboratory [40–42].

Design (a): 4J SCs on InP and InP-on-GaAs Substrates

A detailed discussion of the GaInP/GaAs//GaInAsP/GaInAs SC obtained by bonding on an InP substrate can be found in [43]. The achieved efficiency was 44.7% for C = 297 (AM1.5D). The developed structures were improved: the current matching was attained by changing the photosensitivity of the subcells, the voltage was increased, the serial resistance of the GaInP subcell emitter was decreased, and the optical losses due to contact shadowing were reduced. In the optimized GaInP/GaAs, GaInAsP/GaInAs 4J SC, the InP substrate was replaced by a structurally modified InP (1 μm)-on-GaAs substrate fabricated using the SmartCut technology [29].

The use of this structurally modified substrate reduces the production cost because the bulk (500 μm thick) InP crystal is replaced by a thin (less than 1 μm) layer transferred to an GaAs substrate. In tests of the SCs at the AIST laboratory (Japan), an absolute record of the sunlight conversion efficiency was registered: 46.1% (C = 500, AM1.5D) (Fig. 8a). The values of the photovoltaic parameters indicate the high performance of the semiconductor structures: all subcells of the record-breaking sample have EQE values exceeding 90%, with a good match for the integral photocurrent values, whose spread does not exceed ±2% (Fig. 8b) [29].

The registration and confirmation of absolute records for the radiation conversion efficiency largely depend on the characteristics of the test equipment, primarily, on the accuracy of reproduction of the irradiance and

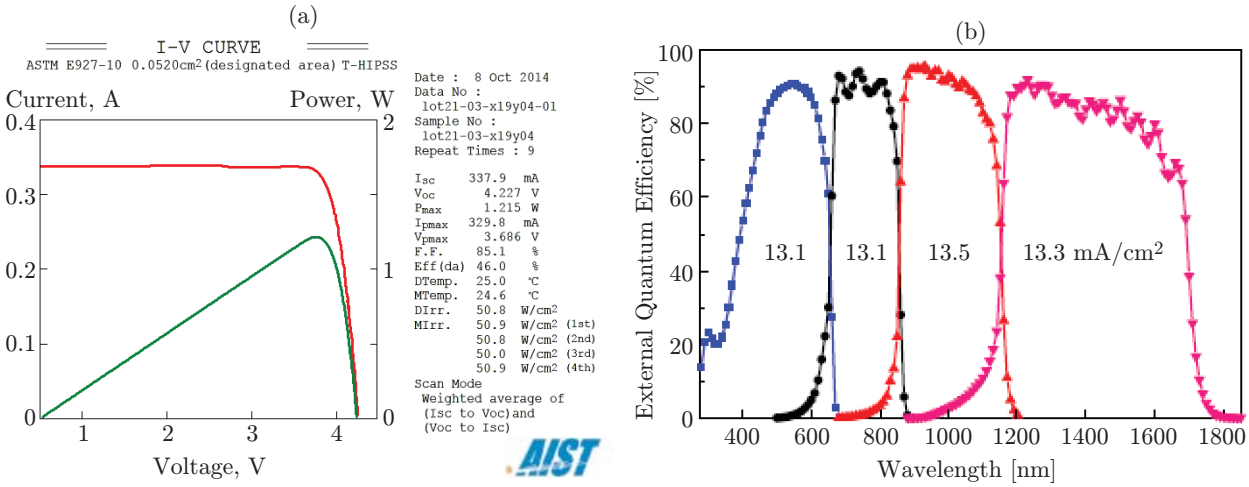

Fig. 8. Results of measurements of a 4J CE on an InP-on-GaAs substrate: (a) I-V curve measured at the AIST laboratory; (b) spectral dependences of EQE and photocurrents of subcells (1000 W/m^2, AM1.5D) [29].

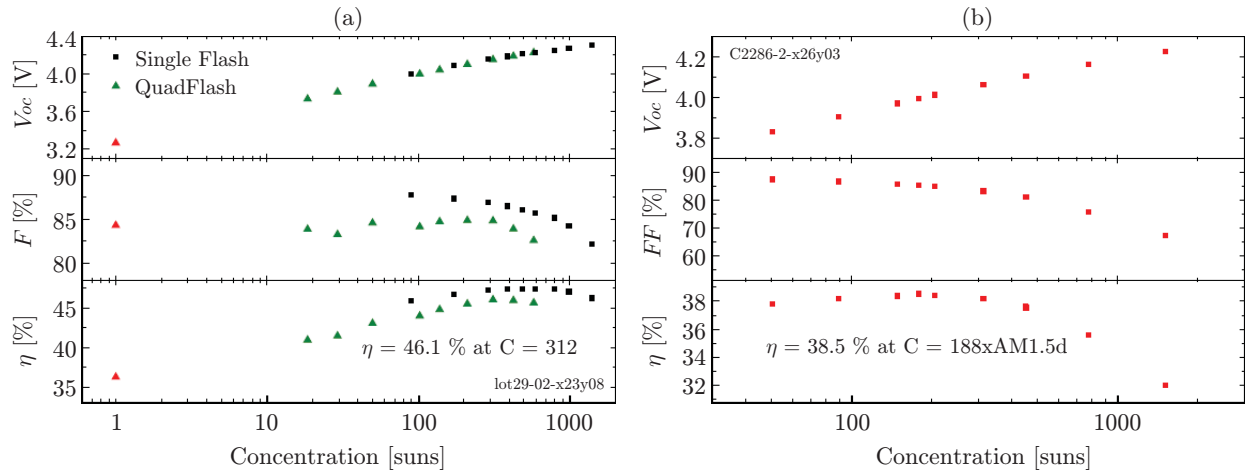

Fig. 9. Photovoltaic parameters versus solar-radiation concentration ratio for 4J SCs: (a) on InP-on-GaAs substrates, (b) on Ge substrates [29].

its spectral density on solar simulators. Comparative measurements have shown a difference of 1.3 abs.% in the SC efficiency (47.4% for C = 389 is set at FhG-ISE against 46.1% for C = 312 at AIST) (Fig. 9a), which is explained by the overestimated photocurrent for the GaInAsP subcell in tests on a single source simulator at FhG-ISE. Using a simulator with a precise tuning of the spectrum (at AIST), almost identical irradiance conditions were created for all four subcells: the current matching mode immediately led to a decrease in FF and hence the SC efficiency. Currently, the value of 46.1% (C = 312, AM1.5D) is the absolute maximum measured efficiency for SCs of all types, which again confirms the importance of the quality of semiconductor materials for such devices and the role of technological art in their development.

Design (b): 4J SCs Based on Active Ge

4J SCs based on active Ge were implemented by a combination of inverted growth for AlGaInP/GaAs 2J SCs and direct metamorphic growth for $Ga_{0.82}In_{0.18}As$/Ge 2J SCs (Fig. 7a). Both structures were bonded by activated surfaces at FhG-ISE. In the developed structure, the greatest attention was paid to the $Ga_{0.82}In_{0.18}As$ material, whose photovoltaic properties strongly depend on the density of threading dislocations on the surface of the metamorphic GaInAs buffer layer. The measured density of threading dislocations was less than 10^6 cm^{-2} and should not have a significant influence on the SC characteristics. Nevertheless, the photocurrent densities in each subcell turned were approximately 1 mA/cm^2 lower than the above

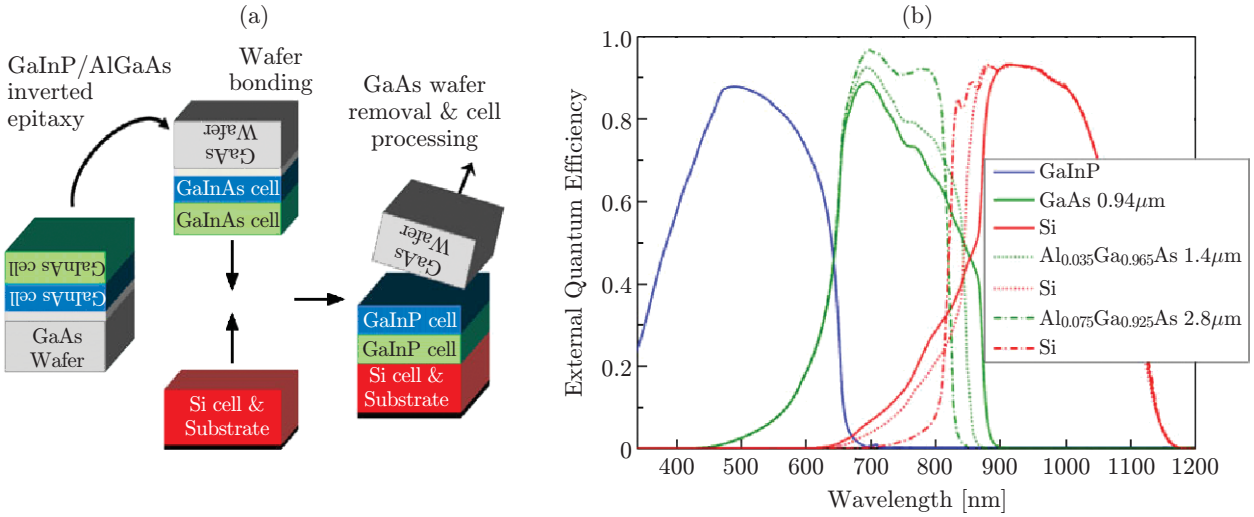

Fig. 10. (a) diagram of the fabrication process for $Ga_{0.51}In_{0.49}P/Al_xGa_{1-x}As$//Si 3J SCs; (b) EQE dependences in the simulation of the absorption in the $GaInP/Al_xGa_{1-x}As$//Si SC structure at an Al content of 0, 3.5, and 7.5 % in the layers of the middle subcell [30].

data for GaInP/GaAs//GaInAsP/GaInAs SCs on a modified InP substrate. Dependences of the I-V curve parameters on the radiation concentration ratio are shown in Fig. 9b: the efficiency does not exceed 38.5% (AM1.5D) for C = 188 because of the high resistance of the bottom tunnel diode and/or the surface corresponding to the sintering boundary and the lower V_{OC} voltage than for the GaInP/GaAs//GaInAsP/GaInAs 4J CE [29].

Design (c): 4J SCs on a GaSb Substrate

In 4J SCs on a GaSb substrate design (see Fig. 7), the inverted metamorphic grown (IMM) top GaInP/GaAs/GaInAs 3J-cascade with a $In_xGa_{1-x}P$ buffer layer between GaAs and $Ga_{0.76}In_{0.24}As$ was connected to a GaSb subcell using surface activated bonding. The top subcells showed an EQE of 85–90%, whereas for narrow-bandgap GaSb, it did not exceed 60%, which is explained by recombination at the interface between the *n*-GaInAs layer and the *n*-GaSb emitter because of the absence of a passivation layer on its surface. This region 2 to 5 nm thick [44, 45] formed before bonding in the activation of the surfaces with argon atoms has high defect density with nonradiative recombination. Improvement of the GaSb subcell design involves the introduction of a transparent passivation layer on the front surface to prevent the transition of minority charge carriers to the bonding interface. The obtained 4J SC demonstrates V_{OC} = 3.9 V and the maximum efficiency of 29.1% for C = 194 [29].

III–V/Si TRIPLE-JUNCTION MONOLITHIC SCs

Various strategies for the formation of III–V SCs on Si have been studied [46, 47]. Solar cells with an efficiency of 27.9% (C = 48, AM1.5D) were obtained on GaAsP/GaAs//Si 3J-structures using bonding technology [11]. The development of bonding technology for 3J SCs based on III–V heterostructures and active silicon is presented in [30]. These SCs were prepared by joining a $Ga_{0.51}In_{0.49}P/Al_xGa_{1-x}As$ 2J monolithic heterostructure with a single-junction Si-structure formed on a float-zone (FZ) *p*-type silicon wafer with an activated surface. The main problems were to optimize the bandgaps of III–V subcells and match their photocurrents with the current of the silicon *p*–*n* junction. A schematic of the process is shown in Fig. 10a.

A cascade comprising two top subcells was fabricated in the LM-configuration with the inverse (first $Ga_{0.51}In_{0.49}P$ layers and then $Al_xGa_{1-x}As$) order of growth on 4-inch GaAs substrates by MOVPE technology [11]. A silicon (narrow-bandgap) subcell was obtained by implantation of phosphorus atoms into *c*-Si (2 Ω · cm, 280 μm) wafers with subsequent high-temperature annealing in an inert atmosphere. The front surfaces of the structures were processed by a flow of argon atoms with an energy of 0.3-0.4 keV at a temperature of 120°C and a pressure of less than $3 \cdot 10^{-8}$ mbar [45], followed by pressing with a force of 10 kN for a few minutes. It has been shown that the *n*-Si//*n*-GaAs interface has sufficient strength, high transparency, and homogeneous conductivity over the entire contact area. The GaAs growth substrate for

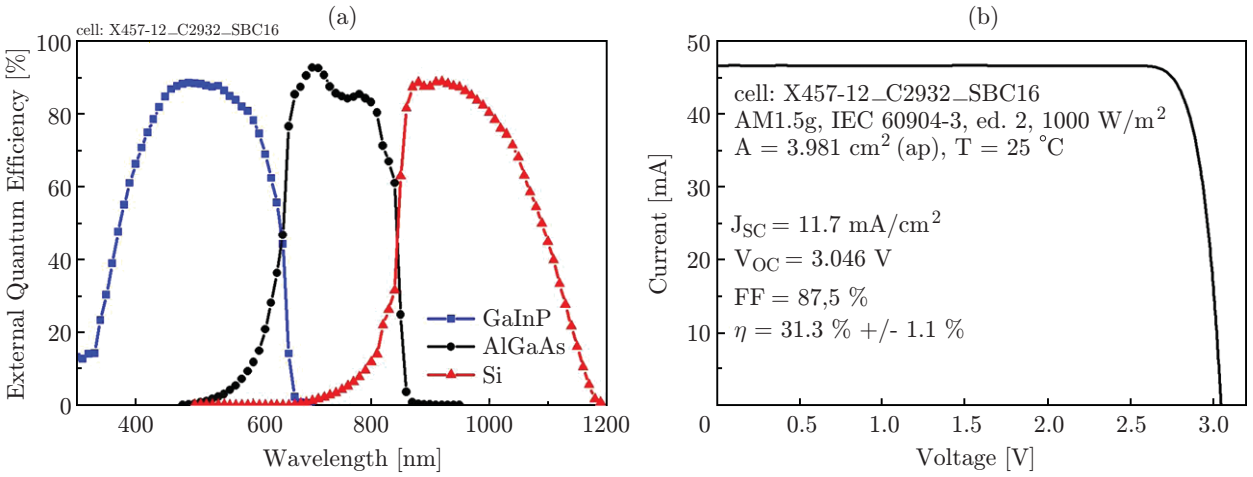

Fig. 11. (a) spectral dependence of EQE; (b) I-V curve for a $Ga_{0,51}In_{0,49}P/Al_xGa_{1-x}As$//Si3J SC with a record-breaking efficiency of 31.3% (AM1.5G) [48].

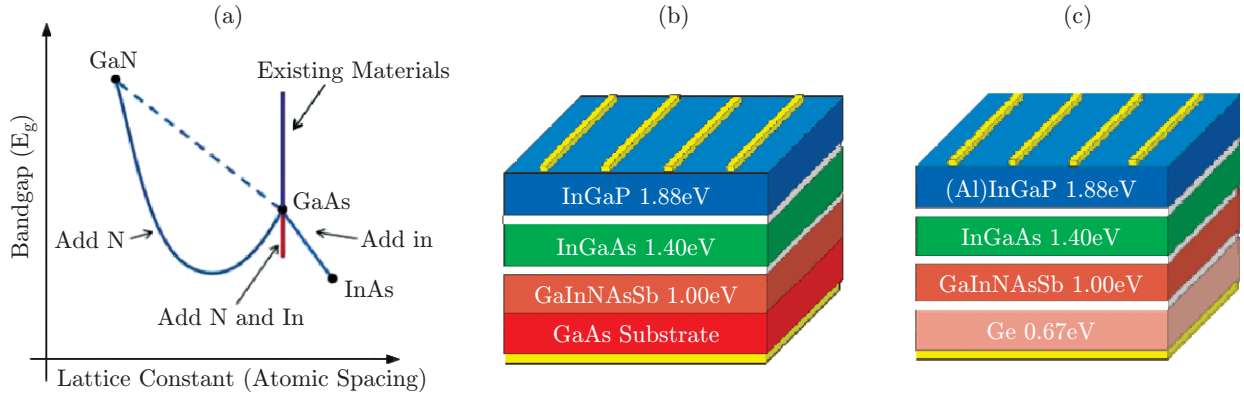

Fig. 12. (a) dependence of the BG width on the lattice constant for GaInNAs compounds [8]; (b, c) 3J and 4J SC architectures, respectively, with a GaInNAsSb *p*–*n* junction (1 eV) [51].

the pair of $Ga_{0.51}In_{0.49}P/Al_xGa_{1-x}As$ subcells was etched in a mixture of $H_2O_2 + NH_4OH$. The optimal architecture for matching the subcell currents was sought by simulation of a 3J SC based on $Al_xGa_{1-x}As$ layers of different thicknesses and with different Al percentages (0, 3.5 and 7.5%) for the middle subcell with a BG width equal to 1.42, 1.47, and 1.52 eV, respectively (Fig. 10b).

It has been established that the lifetime of charge carriers in *c*-Si and the photocurrent density of the Si subcell decrease during chemical etching of the GaAs substrate. The problem was solved by additional etching of Si in HF and by deposition of a AlO_x/SiN_x coating. As a result, the photocurrent density for the Si-subcell was increased to 12.6 mA/cm^2, which corresponds to the target value for the current matching in the $Ga_{0.51}In_{0.49}P/Al_xGa_{1-x}As$//Si SC. However, a perfect matching of the photocurrents has not yet been achieved. In the best GaInP/GaAs//Si sample with an efficiency of 30.2% (C = 1, AM1.5G), there is a limitation on the photocurrent from the middle GaAs subcell [30]. For monolithic III–V/Si SCs, it is planned to increase the BG width for both III–V subcells without deterioration of the quality of semiconductor materials and to improve the Si passivation technology. Developers from FhG-ISE have demonstrated a new record-breaking efficiency of 31.3% for III–V/Si SCs (Fig. 11) [1, 48]. It is believed [30] that in the future the efficiency of III–V/Si SCs will reach 35% (AM1.5G).

TRIPLE- AND FOUR-JUNCTION SCs WITH SUBCELLS BASED ON NITRIDE GaInNAsSb SOLID SOLUTIONS

A solution to the problem of the fabrication of narrow-bandgap GaAs or Ge matched photoactive layers for subcells with a BG width of 0.7 to 1.3 eV is presented by the Solar Junction company (U.S.), which has

developed MBE modes for nitride GaInNAsSb solid solutions with controlled variations in the BG width [8]. Addition of a small amount (several atomic percent) of nitrogen reduces the lattice constant and the BG width of the GaAs (Fig. 12a). At the same time, the addition of indium increases the lattice constant, while decreasing the BG width. By regulating the N and In contents in GaInNAs and maintaining the ratio in the range of about 2.7 to 1, it is possible to change E_g of the solution from 0.7 to 1.3 eV, while maintaining the matching of the lattice constant with Ge.

Numerous efforts using MOCVD technology to obtain GaInNAs solid solutions with suitable characteristics (primarily, the parameters of minority charge carriers) for use in MJ SCs have not led to success [49]. The introduction of hydrogen and carbon increases nonradiative recombination, reduces the diffusion length of minority charge carriers, and, consequently, leads to a drop in the photocurrent and voltage in the SC. For MBE technology, the problem was to control the amount of nitrogen introduced into the growth layers to eliminate the defects acting as centers of nonradiative recombination. For both the MOCVD and MBE processes, poorly controlled introduction of nitrogen into the lattice led to the formation of segregated films, clusters, and interstitial defects [50]. The Solar Junction company has developed an MBE growth process for nitride layers with the addition of antimony as surfactant, which has made it possible to solve above-mentioned problems and produce high-performance GaInNAsSb layers for subcells with a BG width of 0.8-1.3 eV. This range overlaps the important spectral interval between the absorption zones of GaAs and Ge, which can be filled only with metamorphic materials. GaInNAsSb compounds, together with InAlGaP, AlGaAs, and Ge, form a complete set of architectures with the necessary zones for the development of 3J, 4J, 5J, and even 6J SCs.

In the first experiments, the Solar Junction company developed GaInNAsSb subcells with an energy of 0.9–1 eV as a replacement of the Ge-cascade in the classical 3J GaInP/GaInAs/Ge SC. In the developed 3J GaInP/GaAs/GaInNAsSb, the matching of the photocurrents for all three subcells was preserved and a voltage gain of 200 mV was obtained. The triple-junction architecture on a GaAs substrate and a promising 4J-architecture on a Ge p–n junction are shown in Figs. 12b and 12c.

An efficiency of 43.5% (AM1.5D) was recorded for the range C = 400–600 with the efficiency remaining greater than 42% up to C = 1000, which indicates that such cells are promising for use in systems with sunlight concentrators.

Since 2014 the Solar Junction company has carried out a project to develop a commercial GaInP/GaInAs/GaInNAsSb/Ge 4J SC with an efficiency of 33% (AM0) [52]. The goal of the project is to provide the European Space Agency with high-efficiency SCs on inexpensive 6-inch Ge-substrates using nitride technology for narrow-bandgap junctions. The production is divided into two phases according to the technology used: MBE (the growth of nitrides is planned in Singapore) and MOCVD (the production and testing is planned in the European Union) (the project budget is 4 million Euros, the project term is 2.5 years). Advances in the nitride direction suggest the achievement of efficiency of up to 36% (AM0) for 5J and 6J SCs.

Si-Ge-Sn COMPOUNDS ($E_g \sim 1.0$ eV) FOR MULTI-JUNCTION SCs

For narrow-bandgap cascades of MJ SCs, ternary solid solutions based on the IV-th group elements Si-Ge-Sn have been actively developed [16]. An advantage of Si-Ge-Sn compounds is that their BG width can be changed by varying the composition. If Ge is considered as the basis, then with the addition of Si, the BG width of the material will be above 0.66 eV with a simultaneous decrease in the crystal lattice parameter. Conversely, increasing the percentage of Sn in Ge shifts the BG width to the range below 0.66 eV with an increase in the lattice constant. The combination of these three elements makes it possible to obtain Ge lattice-matched compounds with a BG width of 0.5 to 1.2 eV [53]. Thus, they are an alternative to narrow-bandgap nitride GaInNAsSb subcells and metamorphic GaInAs subcells with E_g of about 1.0 and 0.7 eV. For MJ SCs, the Transucent Inc. company (U.S.) has developed a synthesis technology of Ge and Ge-Sn materials and Si-Ge-Sn alloys. The obtained compounds have good structural properties that allow them to be integrated with the existing architectures of III–V solar cells on Ge. Photoluminescence shows that these materials have a long lifetime of minority charge carriers even at room temperature.

Figure 13a shows the efficiency growth dynamics for MJ SCs with the addition of narrow-bandgap Si-Ge-Sn subcells to the standard SC. The estimates were obtained for the absorption model assuming that the loss of minority carriers is only due to nonradiative recombination.The introduction of a subcell with $E_g = 1.03$ eV into the structure increases the efficiency of the MJ SC from about 40% (C = 1) to 55% (C = 1000).

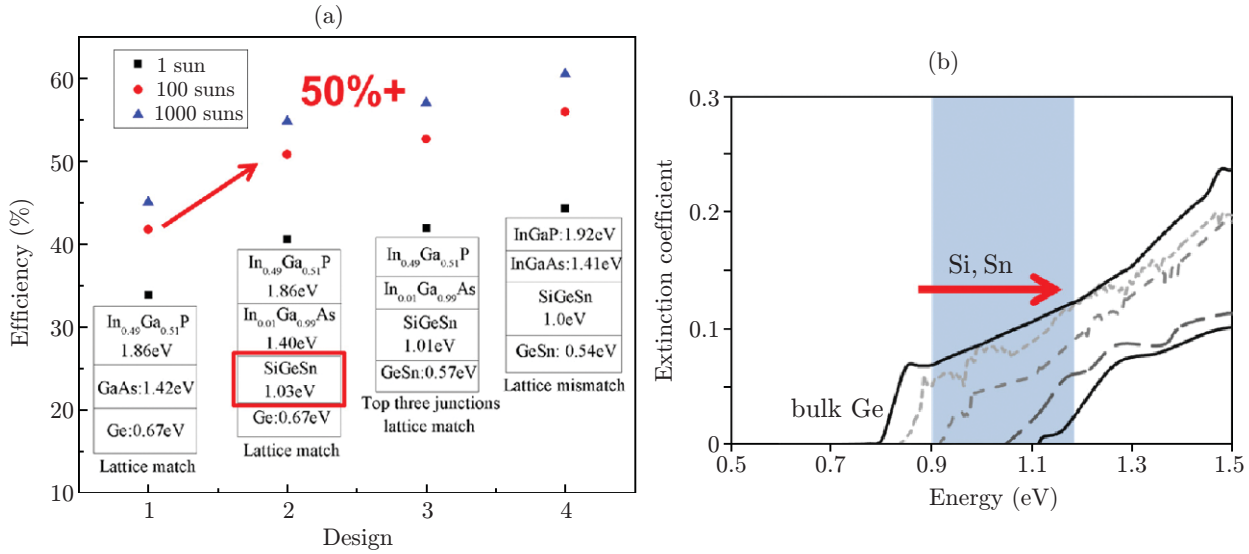

Fig. 13. (a) efficiency growth dynamics for MJ SCs with the addition of narrow-bandgap Si-Ge-Sn subcells into the GaInP/GaInAs/Ge SC architecture; (b) shift of the absorption edge of Si-Ge-Sn with increasing fractions of Si and Sn (range of 0.9–1.1 eV) [16].

Si-Ge-Sn structures were grown by chemical vapor deposition (CVD) [54] at a temperature of 300–450 °C in a horizontal reactor using SnD_4, Si_3H_8 and Ge_2N_6 vapor sources. Growth was carried out on 4-inch Ge(100) substrates disoriented by 6 °C in the [111] direction to form III–V layers without the formation of antiphase domains. The composition of the obtained layers was determined by mass flow control of each component. The density of defects in the layers was far below 10^5 cm^{-2}. The root-mean-square surface roughness was 0.26 nm. The obtained low defect level and atomically smooth surfaces are important for the successful nucleation of subsequent high-performance III–V layers for wide-bandgap subcells. Figure 13b shows the dependences of the BG width on the Si and Sn content in the Si-Ge-Sn structure. It can be seen that as the Si and Sn concentration increase, the absorption edge is gradually shifted toward higher energies. Measurements of the atomic Si and Sn concentrations in the layers using Rutherford backscattering spectroscopy have shown that the Si:Sn ratio is close to 4 : 1 [53]. The Si and Sn concentrations are 8–14% and 2–4%, respectively. Time-resolution photoluminescence showed that the lifetime of charge carriers is approximately 1 ms, which is close to that for III–V alloys on Ge.

The first phase in the production of a III–V/SiGeSn monolithic structure involved the formation of a single-junction GaInAs/SiGeSn/Ge sample (n-emitter/p-base/Ge-substrate) (Fig. 14a). The p-type base was doped with diborane B_2H_6 at a level of $7\cdot10^{17}$–$1\cdot10^{18}$ cm^{-3}. The n-GaInAs emitter (0.25 μm, $5\cdot10^{18}$ cm^{-3}) was formed by diffusion of As or P during thenucleation of layers grown by MOVPE. The SC architecture includes a 30 nm thick layer, which produces an inverse surface field, a Ti/Au contact metal grid, and an Si_3N_4 antireflection coating 65 nm thick.

The current-voltage characteristic (AM1.5G) of a single-stage GaInAs/SiGeSn/Ge SC with a base layer thickness of 1.8 μm and $E_g = 1.0$ eV has a typical diode appearance [16] ($V_{OC} = 0.194$ V, $I_{sc} = 9.4\cdot10^{-3}$ A, $FF = 54.7$ %). The measured EQE level reaches 60%. For the prototype presented in [16], no optimization has been conducted. To date, this is the first operating SC based on a Si-Ge-Sn ternary solid solution.

The GaInAs/SiGeSn/Ge structure is Ge lattice-matched and fully meet the requirements for the manufacture of GaInP/GaInAs/SiGeSn-Ge 3J SCs by the standard technology. A SC sample with the following subcell parameters was manufactured: 0.5 μm GaInP, 1.5 μm GaInAs, and n-GaInAs emitter about 0.25 μm thick.Two GaAs/AlGaAs and GaAs/GaAs tunnel diodes were used for electrical connection of subcells within a monolithic structure.The whole prototype 3J structure was not optimized and served only to prove the concept. Simultaneously, a standard 3J SC was produced for comparison.The following parameter values of the 3J GaInP/GaInAs/SiGeSn-Ge sample were obtained: $V_{OC} = 2.27$ V, $I_{sc} = 1.22\cdot10^{-2}$ A/cm^2, $FF = 82.5$ %, and $P_{max} = 2.5\cdot10^{-2}$ W. For the standard SC under the same conditions, $P_{max} = 3.3\cdot10^{-2}$ W and $FF = 84.1$ %. Analysis of the spectral dependence of the EQE (Fig. 14b) shows that the greatest recombination losses occur at the GaInAs–SiGeSn interface, whose optimization will improve the efficiency of SCs. It has been shown [55] that in the 850–950 nm wavelength range, the EQE for GaInP/GaInAs/SiGeSn-Ge

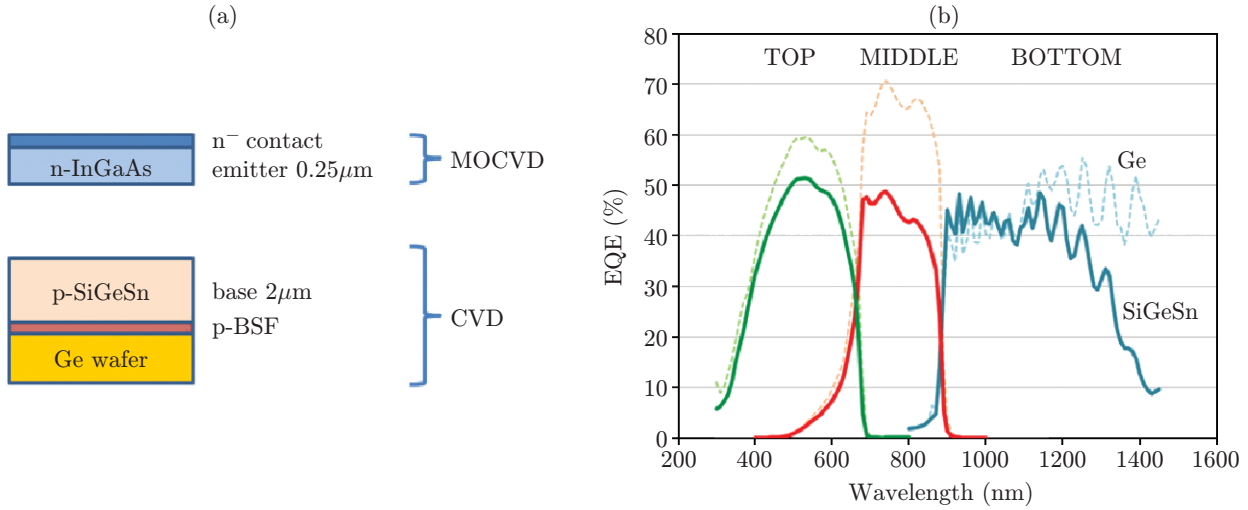

Fig. 14. (a) method of designing the structure and the architecture of a single-junction GaInAs/SiGeSn/Ge sample; (b) EQE for 3J SCs based on GaInP/GaInAs/SiGeSn-Ge structures (solid curves) and GaInP/GaInAs/Ge structures (dashed curves) [16].

SCs increases to 70%, which provides some excess of the photocurrent density over that of the standard GaInP/GaInAs/Ge sample: 13.94 mA/cm^2 and 13.91 mA/cm^2, respectively.

CONCLUSIONS

Multi-junction SCs based on III–V heterostructures provide record-breaking efficiency of sunlight conversion and are superior to all other types of radiant energy converters. The photovoltaic community predicts that the efficiency milestones of 40% (AM0) and 50% (AM1,5D, concentrated radiation) for MJ SCs will be overcome by 2020. To achieve this, a transition from the standard 3J SCs to more efficient 4J-, 5J- and even 6J-architectures is performed and new materials with optimal bandgaps are being improved and created. The first ultra-lightweight flexible 4J SCs based on an inverted metamorphic structure with a record (for the large-scaled production market) efficiency of 32% (AM0) have already appeared on the world market. The developments of bonding technology have provided a record-breaking efficiency of 31.3% for III–V/Si SCs on low-cost and lightweight Si-substrates. The use of bonding together with IMM growth allowed III–V heterostructures to be combined with lattice-mismatched narrow-bandgap InP, Ge, and GaSb materials and to develop the breakthrough MJ SC architectures with a record efficiency of 35.8% (AM0), 38.8% (AM.1.5D) and 46.1% (C = 312, (AM.1.5D). The above-listed high-e?ciency data for conversion of direct and concentrated sunlight were obtained under laboratory conditions. However, as a rule, new developments appear on the market of photovoltaic products within 2–3 years. Based on the developed MBE technology of GaInNAsSb compounds, the project of designing a commercial 4J SC with an efficiency of 33% and with the prospect of its increase to 35% (AM0) and to 47% at concentrated terrestrial sunlight is already underway [56, 57]. Si-Ge-Sn compounds of group IV allowing the BG width to be varied from 0.5 to 1.2 eV while matching the Ge lattice are very new and extremely promising for the development of monolithic MJ SCs with design efficiencies of more than 50% [16].

REFERENCES

1. M. A. Green, Y. Hishikawa, W. Warta, et al., “Solar Cell Efficiency Tables (version 50),” Progress in Photovoltaics: Research and Appl. **25** (7), 668–676 (2017).
2. M. M. Koltun, *Optics and Metrology of Solar Cells* (Nauka, Moscow, 1985) [in Russian].
3. *ISO 15387:2005. Space Systems — Single-Junction Solar Cells — Measurements and Calibration Procedures.*
4. *IEC 60904-3:2016. Photovoltaic Devices. Pt. 3: Measurement Principles for Terrestrial Photovoltaic (PV) Solar Devices with Reference Spectral Irradiance Data.*
5. *ASTM G173-03(2012). Standard Tables for Reference Solar Spectral Irradiances: Direct Normal and Hemispherical on 37° Tilted Surface.*

6. A. W. Bett, S. P. Philipps, S. Essig, et al., "Overview about Technology Perspectives for High Efficiency Solar Cells for Space and Terrestrial Applications," in *Proc. of the 28th Europ. Photovoltaic Solar Energy Conference and Exhibition*, Paris, France, 30 Sept. — 4 Oct., 2013, pp. 1–6.
7. T. Takamoto, H. Washio, and H. Juso, "Application of InGaP/GaAs/InGaAs Triple Junction Solar Cells to Space Use and Concentrator Photovoltaic," in *Proc. of the 40th IEEE Photovoltaic Specialists Conf., Denver*, USA, June 8–13, 2014. P. 0001–0005.
8. V. Sabnis, H. Yuen, and M. Wiemer, "High-Efficiency Multijunction Solar Cells Employing Dilute Nitrides," in *Proc. of the 8th Intern. Conf. on Concentrating Photovoltaic Systems* **1477** (1), 14–19 (2012).
9. S. A. Ringel, J. A. Carlin, C. L. Andre, et al., "Single-Junction InGaP/GaAs Solar Cells Grown on Si Substrates with SiGe Buffer Layers," Progress in Photovoltaics: Research and Appl. **10** (6), 417–426 (2002).
10. K. Derendorf, S. Essig, E. Oliva, et al., "Fabrication of GaInP/GaAs//Si Solar Cells by Surface Activated Direct Wafer Bonding," IEEE J. Photovoltaics **3** (4), 1423–1428 (2013).
11. F. Dimroth, T. Roesener, S. Essig, et al., "Comparison of Direct Growth and Wafer Bonding for the Fabrication of Beam GaInP/GaAs Dual-Junction Solar Cells on Silicon," IEEE J. Photovoltaics **4** (2), 620–625 (2014).
12. J. M. Zahler, K. Tanabe, C. Ladous, et al., "High Efficiency InGaAs Solar Cells on Si by InP Layer Transfer," Appl. Phys. Lett. **91** (1), 012108 (2007).
13. M. J. Archer, D. C. Law, S. Mesropian, et al., "GaInP/GaAs Dual Junction Solar Cells on Ge/Si Epitaxial Templates," Appl. Phys. Lett. **92** (10), 103503 (2008).
14. P. Patel, D. Aiken, A. Boca, et al., "Experimental Results from Performance Improvement and Radiation Hardening of Inverted Metamorphic Multijunction Solar Cells," IEEE J. Photovoltaics **2** (3), 377–381 (2012).
15. D. B. Jackrel, S. R. Bank, H. B. Yuen, et al., "Dilute Nitride GaInNAs and GaInNAsSb Solar Cells by Molecular Beam Epitaxy," J. Appl. Phys. **101** (11), 114916 (2007).
16. R. Roucka, A. Clark, and B. Landini, "Si-Ge-Sn Alloys with 1.0 eV Gap for CPV Multijunction Solar Cells," in *Proc. of the 11th Intern. Conf. on Concentrator Photovoltaic Systems*, **1679** (1), 040008 (2015).
17. W. Guter, J. Schöne, S. P. Philipps, et al., "Current-Matched Triple-Junction Solar Cell Reaching 41.1% Conversion Efficiency under Concentrated Sunlight," Appl. Phys. Lett. **94** (22), 223504 (2009).
18. R. R. King, D. C. Law, K. M. Edmondson, et al., "40% Efficient Metamorphic GaInP/GaInAs/Ge Multijunction Solar Cells," Appl. Phys. Lett. **90** (18), 183516 (2007).
19. D. Aiken, E. Dons, S.-S. Je, et al., "Lattice-Matched Solar Cells with 40% Average Efficiency in Pilot Production and a Roadmap to 50%," IEEE J. Photovoltaics **3** (1), 542–547 (2013).
20. A. B. Cornfeld, M. Stan, T. Varghese, et al., "Development of a Large Area Inverted Metamorphic Multi-Junction (IMM) Highly Efficient AM0 Solar Cell," in *Proc. of the 33rd IEEE Photovoltaic Specialists Conf. San Diego*, USA, 11–16 May, 2008. P. 88 [CD].
21. J. F. Geisz, D. J. Friedman, J. S. Ward, et al.. "40.8% Efficient Inverted Triple-Junction Solar Cell with Two Independently Metamorphic Junctions," Appl. Phys. Lett. **93** (12), 123505 (2008).
22. R. M. France, J. F. Geisz, M. A. Steiner, et al., "Pushing Inverted Metamorphic Multijunction Solar Cells toward Higher Efficiency at Realistic Operating Conditions," IEEE J. Photovoltaics **3** (2), 893–898 (2013).
23. P. Patel, D. Aiken, A. N. Boca, et al., "Experimental Results from Performance Improvement and Radiation Hardening of Inverted Metamorphic Multijunction Solar Cells," IEEE J. Photovoltaics **2** (3), 377–381 (2012).
24. C. Youtsey, J. Adams, R. Chan, et al., "Epitaxial Lift-Off of Large-Area GaAs Thin-Film Multi-Junction Solar Cells," in *Proc. of the CS MANTECH Conf. Boston*, USA, April 23–26, 2012 [CD].
25. H. Moriceau, F. Rieutord, F. Fournel, et al., "Overview of Recent Direct Wafer Bonding Advances and Applications," Adv. Nat. Sci.: Nanosci. Nanotechnol. **1**, 043004 (2010).
26. Q.-Y. Tong and U. Gösele, *Semiconductor Wafer Bonding: Science and Technology* (John Wiley and Sons, New York, 1999).
27. D. C. Law, D. M. Bhusari, S. Mesropian, et al., "Semiconductor-Bonded III-V Multijunction Space Solar Cells," in *Proc. of the 34th IEEE Photovoltaic Specialists Conf. Philadelphia*, USA, June 7–12, 2009, pp. 2237–2239.
28. S. J. Boisvert, D. Law, R. King, et al., "Development of Advanced Space Solar Cells at Spectrolab," in *Proc. of the 35th IEEE Photovoltaic Specialists Conf. Honolulu*, USA, June 20–25, 2010, pp. 000123–000127.
29. F. Dimroth, T. N. D. Tibbits, M. Niemeyer, et al., "Four-Junction Wafer-Bonded Concentrator Solar Cells," IEEE J. Photovoltaics **6** (1), 343–349 (2016).
30. R. Cariou, J. Benick, P. Beutel, et al., "Monolithic Two-Terminal III-V//Si Triple-Junction Solar Cells with 30.2% Efficiency under 1-Sun AM1.5g," IEEE J. Photovoltaics **7** (1), 367–373 (2017).
31. P. T. Chiu, D. C. Law, R. L. Woo, et al., "35.8% Space and 38.8% Terrestrial 5J Direct Bonded Cells," in *Proc. of the 40th IEEE Photovoltaic Specialist Conf. Denver*, USA, June 8–13, 2014, pp. 0011–0013.
32. G. F. X. Strobl, L. Ebel, D. Fuhrmann, et al., "Development of Lightweight Space Solar Cells with 30% Efficiency at End-of-Life," in *Proc. of the 40th IEEE Photovoltaic Specialist Conf.*, Denver, USA, June 8–13, 2014. 3595.

33. N. A. Pakhanov, O. P. Pchelyakov, and V. M. Vladimirov, "Superthin Solar Cells Based on $A^{III}B^{V}$/Ge Heterostructures," Autometriya **53** (6), 106–110 (2017) [Optoelectron., Instrum. Data Process. **53** (6), 625–629 (2017)].
34. N. Miller, P. Patel, C. Struempel, et al., "EMCORE Four-Junction Inverted Metamorphic Solar Cell Development," Proc. of the 10th Intern. Conf. on Concentrator Photovoltaic Systems **1616** (1), 50–53 (2014).
35. M. Stan, D. Aiken, B. Cho, et al., "Evolution of the High Efficiency Triple Junction Solar Cell for Space Power," in *Proc. of the 33rd IEEE Photovoltaic Specialists Conf.*, San Diego, USA, May 11–16, 2008, pp. 1–6.
36. M. Yamaguchi, "Radiation Resistance of Compound Semiconductor Solar Cells," J. Appl. Phys. **78** (3), 1476–1480 (1995).
37. *SolAero Technologies Corp.* https://solaerotech.com/wp-content/uploads/2017/06/IMM-alpha-Preliminary-Datasheet-June-2017.pdf.
38. R. R. King, D. Bhusari, A. Boca, et al., "Band Gap-Voltage Offset and Energy Production in Next-Generation Multijunction Solar Cells," Progress in Photovoltaics: Research and Appl. **19** (7), 797–812 (2011).
39. M. S. Leite, R. L. Woo, J. N. Munday, et al., "Towards an Optimized All Lattice-Matched InAlAs/InGaAsP/InGaAs Multijunction Solar Cell with Efficiency >50%," Appl. Phys. Lett. **102** (3), 033901 (2013).
40. C. R. Osterwald and G. Siefer, "CPV Multijunction Solar Cell Characterization," in *Handbook of Concentrator Photovoltaic Technology*, Ed. by C. Algora and I. Rey-Stolle (John Wiley & Sons, 2016), pp. 589–614.
41. V. D. Rumyantsev, V. M. Andreev, V. R. Larionov, et al., "Indoor Characterization of Multijunction Concentrator Cells under Flash Illumination with Variable Spectrum," in *Proc. of the 4th ICSC. El Escorial*, Spain, 2007, pp. 277–280.
42. M. Schachtner, M. L. Prado, S. K. Reichmuth, et al., "Analysis of a Four Lamp Flash System for Calibrating Multi-Junction Solar Cells under Concentrated Light," in *Proc. 11th Intern. Conf. on Concentrator Photovoltaic Systems*, **1679** (1), 050012 (2015).
43. F. Dimroth, T. N. D. Tibbits, P. Beutel, et al., "Development of High Efficiency Wafer Bonded 4-Junction Solar Cells for Concentrator Photovoltaic Applications," in *Proc. of the 40th IEEE Photovoltaic Specialist Conf. Denver*, USA, June 8–13, 2014, pp. 0006–0010.
44. S. Essig and F. Dimroth, "Fast Atom Beam Activated Wafer Bonds between n-Si and n-GaAs with Low Resistance," ECS J. Solid State Sci. Technol. **2** (9), Q178–Q181 (2013).
45. S. Essig, O. Moutanabbir, A. Wekkeli, et al., "Fast Atom Beam-Activated n-Si/n-GaAs Wafer Bonding with High Interfacial Transparency and Electrical Conductivity," J. Appl. Phys. **113**, 203512 (2013).
46. T. Roesener, H. Döscher, A. Beyer, et al., "MOVPE Growth of III-V Solar Cells on Silicon in 300 mm Closed Coupled Showerhead Reactor," in *Proc. of the 25th Europ. Photovoltaic Solar Energy Conference and Exhibition*, Valencia, Spain, Sept. 6–10, 2010, pp. 964–968.
47. M. Yamaguchi, K.-H. Lee, K. Araki, et al., "Potential and Activities of III-V/Si Tandem Solar Cells," ECS J. Solid State Sci. Technol. **5** (2), Q68–Q73 (2016).
48. *Fraunhofer Institute for Solar Energy Systems ISE.* https://www.ise.fraunhofer.de/en/press-media/news/2017/31-3-percent-efficiency-for-silicon-based-multi-junction-solar-cell.html.
49. F. Dimroth, C. Baur, A. W. Bett, et al., "Comparison of Dilute Nitride Growth on a Single- and 8 × 4-inch Multiwafer MOVPE System for Solar Cell Applications," J. Crystal Growth. **272** (1–4), 726–731 (2004).
50. A. J. Ptak, S. Kurtz, S. W. Johnston, et al., "Defects in GaInNAs: What We've Learned so Far," in *Proc. of the Conf. of National Center for Photovoltaics and Solar Program Review Meeting. Denver*, USA, March 24–26, 2003, pp. 1–4.
51. F. Suarez, T. Liu, A. Sukiasyan, et al., "Advances in Dilute Nitride Multi-Junction Solar Cells for Space Power Applications," in *Proc. of 11th ESPC, E3S Web of Conf.* **16**, 03006 (2017).
52. A. P. Kirk, "High Efficacy Thinned Four-Junction Solar Cell," Semicond. Sci. Technol. **26**, 125013 (2011).
53. Y.-Y. Fang, J. Xie, J. Tolle, et al., "Molecular-Based Synthetic Approach to New Group IV Materials for High-Efficiency, Low-Cost Solar Cells and Si-Based Optoelectronics," J. Amer. Chem. Soc. **130** (47), 16095 (2008).
54. J. Xie, J. Tolle, V. R. D'Costa, et al., "Direct Integration of Active $Ge_{1-x}(Si_4Sn)_xGe_{1-x}(Si_4Sn)_x$ Semiconductors on Si(100)," Appl. Phys. Lett. **95** (18), 181909 (2009).
55. T. Wilson, T. Thomas, M. Führer, et al., "Single and Multi-Junction Solar Cells Utilizing a 1.0 eV SiGeSn Junction," in *Proc. of the 12th Intern. Conf. on Concentrator Photovoltaic Systems*, **1766** (1), 060006 (2016).
56. A. Aho, A. Tukiainen, V. Polojärvi, and M. Guina, "Dilute Nitride Space Solar Cells: Towards 4 Junctions," in *Proc. of the 10th Europ. Space Power Conf. Noordwijkerhout*, the Netherlands, **719**, 1–3 (2014).
57. M. Ochoa, I. Garcia, I. Lombardero, et al., "Advances Towards 4J Lattice-Matched Including Dilute Nitride Subcell for Terrestrial and Space Applications," in *Proc. of the 43rd IEEE Photovoltaic Specialists Conf.*, Portland, USA, 2016, pp. 0052–0057.